



King Saud University
Journal of Saudi Chemical Society

www.ksu.edu.sa
www.sciencedirect.com

**ORIGINAL ARTICLE**

Efficient chromium abstraction from aqueous solution using a low-cost biosorbent: *Nauclea diderrichii* seed biomass waste



Martins O. Omorogie ^{a,b}, Jonathan O. Babalola ^{b,*}, Emmanuel I. Unuabonah ^{c,d}, Weiguo Song ^e, Jian Ru Gong ^{a,*}

^a National Center for Nanoscience and Technology, 11 Zhongguancun Beiyitiao, Beijing 100190, People's Republic of China

^b Department of Chemistry, University of Ibadan, Ibadan, Nigeria

^c Department of Chemical Sciences, Redeemer's University, Ogun State, Nigeria

^d Institut für Chemie, Universität Potsdam, Germany

^e Institute of Chemistry, Chinese Academy of Sciences, Beijing, People's Republic of China

Received 7 March 2012; accepted 30 September 2012

Available online 10 November 2012

KEYWORDS

Biomass;
Equilibrium;
External mass transfer;
Kinetics;
Adsorption;
Water

Abstract Toxic Cr(III) which poses environmental hazard to flora and fauna was efficiently abstracted by low-cost *Nauclea diderrichii* seed biomass (NDS) with good sequestrational capacity for this metal was investigated in this study.

The NDS surface analyses showed that it has a specific surface area of 5.36 m²/g and pH_{pzc} of 4.90. Thermogravimetric analysis of NDS showed three consecutive weight losses from 50–200°C (ca. 5%), 200–400°C (ca. 35%), >400°C (ca. 10%), corresponding to external water molecules, structural water molecules and heat induced condensation reactions respectively. Differential thermogram of NDS presented a large endothermic peak between 20–510°C suggesting bond breakage and dissociation with the ultimate release of small molecules.

The experimental data showed kinetically fast biosorption with increased initial Cr(III) concentrations, indicating the role of external mass transfer mechanism as the rate controlling mechanism in this adsorption process. The Langmuir biosorption capacity of NDS was 483.81 mg/g. The use of the corrected Akaike Information Criterion tool for ranking equilibrium models suggested that the Freundlich model best described the experimental data, which is an indication of the heterogeneous nature of the active sites on the surface of NDS.

* Corresponding authors. Tel.: +234 803 454 0881 (J.O. Babalola), +86 10 82545649 (J.R. Gong).

E-mail addresses: bamijibabalola@yahoo.co.uk (J.O. Babalola), gongjr@nanoctr.cn (J.R. Gong).

Peer review under responsibility of King Saud University.



Production and hosting by Elsevier

N. diderrichii seed biomass is an easily sourced, cheap and environmental friendly biosorbent which will serve as a good and cost effective alternative to activated carbon for the treatment of polluted water and industrial effluents.

© 2012 King Saud University. Production and hosting by Elsevier B.V. All rights reserved.

1. Introduction

Chromium pollution problem serves as one of the most serious toxic metal pollution problems in the globe, which has attracted increasing attention of researchers due to vast advancement in global industrialization (Jacobs and Testa, 2004). Toxic metals have become a menace to man, terrestrial and aquatic biota, and to a very great extent hamper ecological sustainability. It is well known that chromium compounds are widely used in various industries, such as leather tanning, paints and pigments, mining, electroplating, and steel fabrication. The industrial wastewater from these processes contains a colossal amount of chromium pollutant that is harmful to the ecological system and human health. Researchers have reported that exposure to a certain level of chromium is responsible for lung cancer, chrome ulcers, nasal septum perforation, as well as brain damage (Chen et al., 2009; Bayramoğlu and Arica, 2008). Many countries have established strict regulations for controlling the release of chromium into the environment. In natural waters, the range of chromium concentration found is in the range of 5.2–208,000 mg/L (Bayramoğlu and Arica, 2008).

Various research studies have shown that toxic metal ions can be removed from aqueous solutions by the biosorption process in batch or continuous mode operations on the laboratory scale, which can be considered to be ideal for large scale treatment of effluents containing toxic metals (Garcia-Reyes and Rangel-Mendez, 2010).

Biosorption of Cr(III) pollutants has been studied using biosorbents of natural origin. Most of these natural biosorbents (which are mostly cellulose based materials) are cost effective, relatively abundant and ubiquitous in the environment. The emergence of biosorption made it possible to utilize various biological substances, such as, palm flower (Elangovan et al., 2008a), rice bran (Oliveira et al., 2005), saltbush leaves (Sawalha et al., 2006), hazelnut shell (Cimino et al., 2000), *Agave lechuguilla* (Romero-Gonzalez et al., 2005), *Leersia hexandra* (Li et al., 2009), *Cassia fistula* and pretreated *C. fistula* (Abbas et al., 2008), *Opuntia ectodermis* (Barrera et al., 2006), and *Citrus reticulata* (Zubair et al., 2008), for the removal of Cr(III) from water and wastewaters.

In recent times, modern techniques such as solid phase extraction (Rajesh et al., 2007, 2008) and nanoscavenging (Howard and Khadry, 2005; Khadry and Howard, 2011; Khadry et al., 2012) have been utilized to adsorb pollutants such as toxic metals and organics from the environment.

N. diderrichii (*De wild*) is a deciduous tree and one of the few indigenous species available in Nigeria which thrives excellently under plantation management in the humid tropical rainforest zone of south-western Nigeria. It is a hard wood with good strength as timber and its resistance to termites makes it essentially valuable to the furniture, art, building and construction industries in West Africa. It is produced in

large commercial scale, which is in hundreds of tons annually (Adeoye and Waigh, 1983; IUCN, 1998).

The bark is known to be used locally in the treatment of gonorrhea, stomach pains, fever and sometimes diarrhea. The extraction of secoiridoid and triterpenic acids from the stems of *N. diderrichii* has been reported (Adeoye and Waigh, 1983).

N. diderrichii seed is relatively abundant in Nigeria and some West African countries (IUCN, 1998). Its seed has an outer covering (epicarp) that is discarded as a waste when the tree is being planted. Hence this biomass from the seed is allowed to rot in plantations and forest research institutes where its seedlings are grown, thereby increasing environmental pollution that serves as a menace to lives and biota. However, literature survey has shown that there is currently a dearth of information concerning the use of *N. diderrichii* seed biomass (NDS) for biosorption purpose.

This study reports for the first time, the use of *N. diderrichii* seed biosorbent (NDS) in sequestering Cr(III) ion from aqueous solution. This study further considers, the kinetic and equilibrium dynamics of the biosorption of Cr(III) ions onto *N. diderrichii*.

2. Experimental

2.1. Analytical reagents

The respective salts, $\text{Cr}(\text{NO}_3)_3 \cdot 9\text{H}_2\text{O}$ (>99% purity) and KNO_3 (>98% purity), were purchased from Beijing Chemical Works Company. Anhydrous NaOH (>98% purity), and concentrated HNO_3 (>70% purity) were also purchased from Beijing Chemical Works Company. All these chemicals were used without further purification.

The stock solution of 1000 mg/L of Cr(III) was prepared by dissolving an accurately weighed amount of $\text{Cr}(\text{NO}_3)_3 \cdot 9\text{H}_2\text{O}$ in deionized water that was obtained from the Millipore water instrument. This stock solution was diluted to various working concentrations when needed.

2.2. Preparation of *N. diderrichii* seed biomass (NDS)

N. diderrichii seed biomass (NDS) was obtained from the Forest Research Institute of Nigeria (FRIN), in Ibadan (7° 23' 16" North, 3° 53' 47" East), Nigeria, West Africa. After collection, this seed biomass was dried in an oven at 60°C for 3 h. Thereafter, it was pulverized and sieved to 450 µm particle size which was used in this research.

2.3. Physicochemical characterization of NDS

The NDS biosorbent was characterized using the Perkin Elmer Spectrum 1 Fourier Transform Infra red (FTIR) spectrometer

in conjunction with potassium bromide, KBr wafer, and Scanning Electron Microscope (SEM) (Hitachi S4800 model), Nitrogen sorption-desorption was carried using BET specific surface area analyzer, Micromeritics Instrument Corporation, ASAP 2020 Model analyzer (for specific surface area measurement), X-ray Diffractometer (XRD) (D/Max-2500, Rigaku, Japan) with Cu K α radiation. The Differential Scanning Calorimeter (DSC) and Thermogravimetric/Differential Thermal Analyzer (TG/DTA) both of the Perkin Elmer model were further used to characterize the NDS biosorbent.

The pH_{pzc} (pH at the point of zero charge) was determined using the solid addition method as described by Stumm and Morgan (1996).

2.4. Biosorption Studies

Fifty milligrams each of *N. diderrichii* seed biomass (NDS) was weighed into various 3 mL plastic containers. Stock solution of 1000 mg/L was prepared by dissolving accurately weighed amounts of Cr(NO₃)₃·9H₂O in de-ionized water prepared by the Milli-Q water deionizer. Various experimental solutions were prepared by diluting the stock solutions to the desired concentrations when needed.

The pH_{pzc} study was carried out using 100 mg of NDS biomass in 50 mL of 200 mg/L solution of Cr(III). The pHs of solutions were adjusted to values ranging from 3.0 to 7.0 using either 0.1 M HNO₃ or NaOH. The mixtures were equilibrated in a thermostatic shaker (THZ-C Chinese Model) at 125 rpm for 180 min at room temperature (298 K). At equilibrium, the suspensions were filtered and pure supernatant liquid obtained was analyzed for the residual Cr(III) ion concentration.

Kinetic study was conducted between 0.5 and 120 min in which 20 mL of 20, 40 and 80 mg/L of Cr(III) solution was measured into a set of 100 mL conical flasks containing 50 mL of aqueous solution and 20 mg of NDS biosorbent, and 100 mg of NDS biosorbent was added to 50 mL of 200 mg/L of Cr(III) solution and agitated between 10 and 180 min.

For equilibrium study, 50 mL of Cr(III) with initial concentrations between 200 and 1000 mg/L was contacted with 100 mg of NDS and these suspensions were agitated at 125 rpm for 180 min. All experimental solutions for kinetic and equilibrium studies were adjusted to pH 7, which was the maximum biosorption pH value obtained from initial pH studies.

Effect of biosorbent dose was studied by agitating 50 mL of 200 mg/L of Cr(III) with 100–500 mg of NDS for 180 min at room temperature (298 K). After biosorption study, Cr(III) loaded *N. diderrichii* seed biomass (NDS) was dried in an oven for 6 h at 120 °C.

At equilibrium the suspensions were filtered using filter paper and pure supernatant liquids obtained were taken for the residual Cr(III) ion concentration in the solutions using Perkin Elmer Optima 5300DV Model of ICP-OES (Inductively Coupled Plasma-Optical Emission Spectrometer). The amount of Cr(III) adsorbed was calculated by difference using;

$$q_e = \frac{(C_o - C_e)V}{W} \quad (1)$$

where C_o is the initial concentration of metal ion (mg/L), C_e is the equilibrium concentration of residual metal ion in the solution (mg/L), V is the volume (L) of the aqueous solution

containing metal ions, W is the weight of biosorbent (g) and q_e is the amount of metal ion adsorbed by the biosorbent (mg/g). These suspensions were agitated with a thermostatic shaker (THZ-C Chinese Model) at 125 rpm.

2.4.1. Data modeling

The optimization design for the adsorption system involves the modeling of the experimental data obtained for the removal of Cr(III) ions from aqueous solution by NDS. It is therefore significant and noteworthy to establish the most appropriate equilibrium and kinetic models that describe experimental data obtained; hence the experimental data were fitted into six equilibrium and five kinetic models as shown below using Microsoft Excel Solver Add-On software (see Supporting document for theory of equilibrium and kinetic models).

2.4.2. The Akaike Information Criterion (AIC)

The AIC developed by Akaike (1974) is a methodology for model ranking in a situation where more than one model has been fitted to the data (Gayawan et al., 2010). The general form for calculating the AIC is given as:

$$AIC = 2k - 2\ln(L) \quad (2)$$

where k is the number of parameters in the model and L is the maximum value of the likelihood function for the model. With the assumption that the model errors are normally and independently distributed with n as the number of data points and SSR the sum of squares for the residual, AIC becomes (Bozdogan, 2009).

$$AIC = 2k - n \left[\ln \left(\frac{SSR}{(n-k)} \right) \right] \quad (3)$$

where k is defined in Eq. (2).

When the number of observations (n) is small, Burnham and Anderson (2004) and Mutua (1994) defined a bias-adjustment or correction for the AIC as:

$$AIC_C = AIC + \left[\frac{2k(k+1)}{n-k-1} \right] \quad (4)$$

where k and n are defined in Eqs. (2) and (3) respectively. Since AIC_C converges to AIC as n tends to infinity, Burnham and Anderson (2004) recommended that AIC_C should be used in place of AIC regardless of the number of observations (n).

To quantify the plausibility of each model as being the most appropriate for describing experimental data, we need an estimate of the likelihood of our model.

Now, let

$$\Delta_i = AIC_{C_i} - \min AIC_C \quad (5)$$

where Δ_i is the difference between the AIC_C of the best fitting model and that of model i , AIC_{C_i} is AIC_C for model i , $\min AIC_C$ is the minimum AIC_C value of all models. Then, $L(\text{model}/\text{data}) \propto \exp(-\frac{1}{2}\Delta_i)$ where $\exp(-\frac{1}{2}\Delta_i)$ is the relative likelihood of the model given in the data. Normalizing the relative likelihood values gives:

$$\lambda_i = \frac{\exp(-\frac{1}{2}\Delta_i)}{\sum_{i=1}^R \exp(-\frac{1}{2}\Delta_i)} \quad (6)$$

where λ_i is the Akaike weight for the i th model, given from 1 to R (Burnham and Anderson, 2004).

The model for which AIC_C is least is chosen as the most appropriate model that better describes the experimental data obtained. Akaike's general approach allows for ranking and identification of the best model for describing experimental data from adsorption reactions (Akpa and Unuabonah, 2011).

3. Results and discussion

3.1. Characterization of biosorbent

3.1.1. Point of zero charge (pHpzc)

The pH at the point of zero charge (pHpzc) is the pH at which the amount of negative charges on the biosorbent surface is equal to the amount of positive charges. This is also the pH at which there is net zero charge on the surface of the biosorbent before biosorption. The organic functional groups on the biosorbent surface may acquire a negative or positive charge depending on the solution pH. At pH values higher than the pHpzc, the sites are mainly in dissociated form and acquire a negative charge, while at pH values lower than the pHpzc of these groups, the sites will be in the associated form with a proton to become positively charged (Ofomaja et al., 2009).

Fig. 1 shows the graphical representation of the pHpzc plot of the NDS biosorbent. The pHpzc of NDS biosorbent was found to be 4.90 in the presence of 0.1 M KNO_3 . The pHpzc value of this biosorbent is similar to that obtained by some authors in their previous works, such as 4.40 for untreated coffee waste (Oliveira et al., 2008) and 4.50 for the biomass of *Thuja orientalis* (Malkoc, 2006).

3.1.2. Scanning Electron Microscopy (SEM) and Brunauer–Emmett–Teller (BET) analysis

The SEM images showed that the particles of this biosorbent were relatively large, irregularly shaped, with its surface pores scattered and unevenly distributed while pore visibility increased with decreasing magnification. The SEM images are shown in Fig. S1 in the Supporting document. The BET nitrogen sorption–desorption isotherm graphical representation of NDS biosorbent (is shown in Fig. 2). BET analysis of NDS suggests that it has a specific surface area of $5.36 \text{ m}^2/\text{g}$, with a molecular cross-sectional area and average pore volume

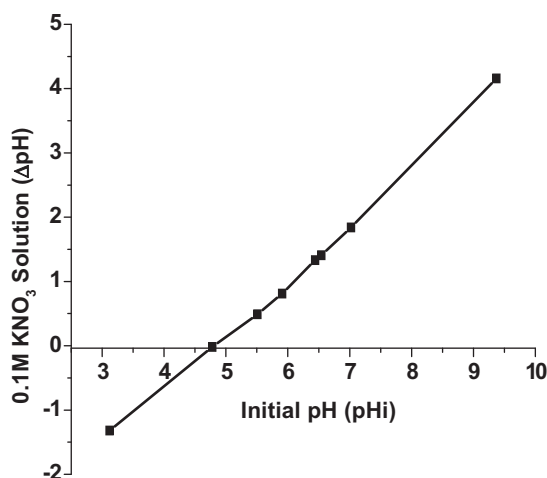


Figure 1 The pH point of zero charge (pHpzc) of NDS biosorbent.

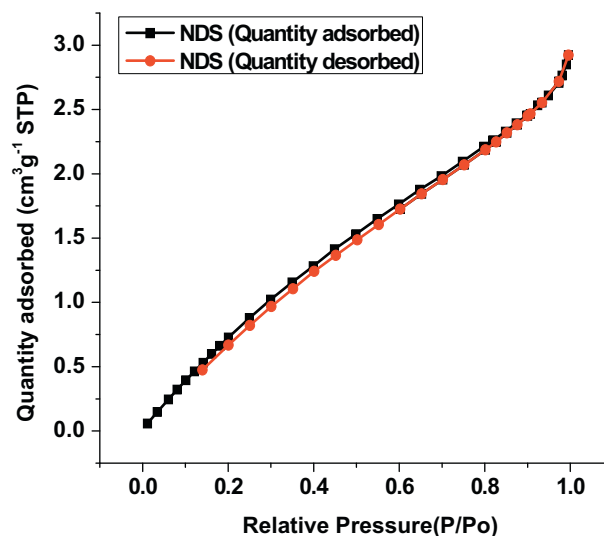


Figure 2 The Brunauer–Emmett–Teller (BET) nitrogen sorption–desorption isotherm graph of quantity adsorbed against the relative pressure of *N. diderrichii* seed biomass (NDS).

of 0.162 nm^2 and $0.00632 \text{ cm}^3/\text{g}$ respectively. The average pore diameter from is 3.986 nm .

The low specific surface area and pore volumes are characteristic of agrowaste (Garcia-Reyes and Rangel-Mendez, 2010). Garcia-Reyes and Rangel-Mendez (2010) reported in their study the use of various agro-wastes as biosorbents for Cr(III) removal. The BET data obtained in this study indicate that NDS biosorbent has pores with relatively good width, but poor pore volume suggesting that much of the biosorption on this biosorbent will be by surface reaction mechanism rather than by pores. Furthermore, the biosorbent might not be very useful in the removal of non-ionic pollutants or molecular pollutants from aqueous solutions like benzene, toluene and xylene.

3.1.3. FTIR spectroscopic analyses

The FTIR spectra of NDS and Cr(III) loaded NDS are shown in Fig. S2 in the Supporting document. The FTIR spectrum of the NDS biosorbent showed a strong peak at 3422 cm^{-1} representing $-\text{OH}$ stretch of cellulose and an $-\text{NH}$ stretch of amine at 3391 cm^{-1} (Kang et al., 2008). The range of $-\text{OH}$ stretch vibrations found around $3420\text{--}2920 \text{ cm}^{-1}$ indicate that this biosorbent predominantly contains cellulose and lignin (Sidiaras et al., 2011). Absorptions at $2945\text{--}2937 \text{ cm}^{-1}$ are for $-\text{C}-\text{H}$ of $-\text{CH}_2$ and $-\text{CH}_3$ stretch vibrations of long polysaccharide chains (Kang et al., 2008). The presence of $-\text{C}=\text{S}$ and $-\text{N}=\text{C}$ stretch vibrations for glycosamine bonds in cellulose and pectin was observed around $2905\text{--}2880 \text{ cm}^{-1}$ and $2860\text{--}2820 \text{ cm}^{-1}$ respectively. Absorption band at 1731 cm^{-1} suggests the presence of carbonyl ($-\text{C}=\text{O}$) functional group. The peak at 1453 cm^{-1} is a stretching vibration for $-\text{C}=\text{C}-$ of olefins. The bending vibrations at 1260 cm^{-1} and 1060 cm^{-1} are peaks for $-\text{C}-\text{O}$ and $-\text{C}-\text{S}$ from phenolic and ether groups in cellulose respectively (Kang et al., 2008). The peaks around the fingerprint region (776 , 705 and 613 cm^{-1}) are out of plane bending vibrations for $-\text{C}-\text{H}$, $-\text{C}-\text{C}-$ and $-\text{HC}=\text{CH}-$ in aromatic compounds (Gobi et al., 2011). The presence of $-\text{C}=\text{O}$, $-\text{OH}$, $-\text{NH}$ functional groups in the NDS biosorbent act as potential active sites for the biosorption of Cr(III).

For Cr(III) loaded NDS, the broad $-OH$ and $-NH$ peaks at $3420\text{--}2920\text{ cm}^{-1}$ were still obvious, indicating that the NDS biosorbent is cellulosic and lignin based. But there was a shift in the vibrational frequency of $-OH$ and $-NH$ from $3420\text{--}2920$ to $3575\text{--}2970\text{ cm}^{-1}$, which suggests that Cr(III) may be bound to $-OH$ and $-NH$ functional groups on NDS via complexation mechanism (Rafatullah et al., 2009). Again, there were observed small shifts in the vibrational frequency of peaks at 1731 cm^{-1} and 1453 cm^{-1} to 1719 cm^{-1} and 1442 cm^{-1} when Cr(III) was loaded on the NDS biosorbent.

3.1.4. X-ray diffraction analyses

The XRD gives information about the change(s) in the crystalline and amorphous portions of NDS. Broad but weak characteristic diffraction peaks at $2\theta = 21^\circ$ and 34° suggest the amorphous nature of the biosorbent (Kobya et al., 2005). The amorphous nature of the NDS biosorbent suggests that Cr(III) could easily penetrate into its surface (Vinod et al., 2010). Fig. S3 in the Supporting document shows the XRD spectrum of NDS.

3.1.5. Differential Scanning Calorimetry (DSC), Thermogravimetry (TG) and Differential Thermal Analysis (DTA)

This is used to investigate the transformational behavior of crystal materials and the heat flow through such materials (Elangovan et al., 2008b). From DSC, NDS adsorbent showed an endothermic peak responded to heat flow from 11 to 15 mW, at a constant temperature of 25°C . Thereafter, heat flow began to increase from 15 to 21 mW with a rise in temperature from 25 to 90°C and dropped from 21 to 18 mW as the temperature rose from 90 to 150°C . The decrease in heat flow through NDS is typical of lignocellulosic materials due to their amorphous nature (Elangovan et al., 2008a).

With TG analysis, there was weight loss of about 5% from 50 to 200°C , 35% from 200 to 400°C and 10% from $>400^\circ\text{C}$ which can be assigned to loss in surface water, structural $-OH$ and heat induced condensation reactions (Eren et al., 2011; Kwon and Castald, 2008; Zhan et al., 2011). This large weight loss by the NDS biosorbent is largely due to its organic nature. For DTA, NDS biosorbent showed a large endothermic peak at $20\text{--}510^\circ\text{C}$ with a corresponding increase in heat flow. This may be due to bond breakage and dissociation of carboxyl, sulphhydryl, amino groups to release of small molecules like CO , H_2S and NH_3 (Kwon and Castald, 2008). Figs. S4a and 4b in the Supporting documents show the DSC, DTA and TG thermograms of NDS.

3.2. Effect of pH

Fig. 3 shows the effect of pH of the solution on the biosorption of Cr(III) ions onto NDS biosorbent, Cr(III) biosorbed increased with increase in pH of aqueous solution. Increasing Cr(III) ion biosorption with increasing pH indicates the presence of fewer H^+ ions at higher pH conditions that could compete with the Cr(III) cations for the available active sites on the NDS biosorbent. Similar results have been obtained by Anirudhan and Radhakrishnan (2007).

At $\text{pH} > 4.9$ (pH_{pzc}), the surface of the NDS biosorbent becomes negatively charged. Under this condition more Cr(III) ions will be adsorbed onto the NDS biosorbent

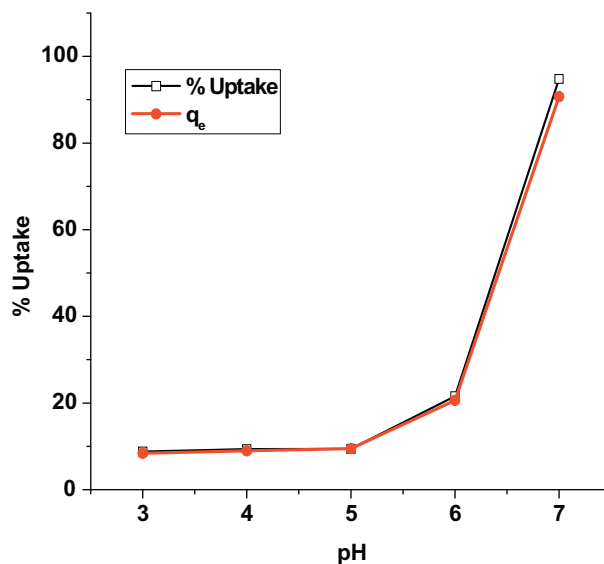


Figure 3 Percent uptake of Cr(III) ion against pH and the amount of Cr(III) ion biosorbed q_e (mg/g) against pH. (Initial metal ion concentration: 200 mg/L, biosorbent dose: 100 mg, temperature: 298 K, agitation time: 3 h, agitation speed: 125 rpm.)

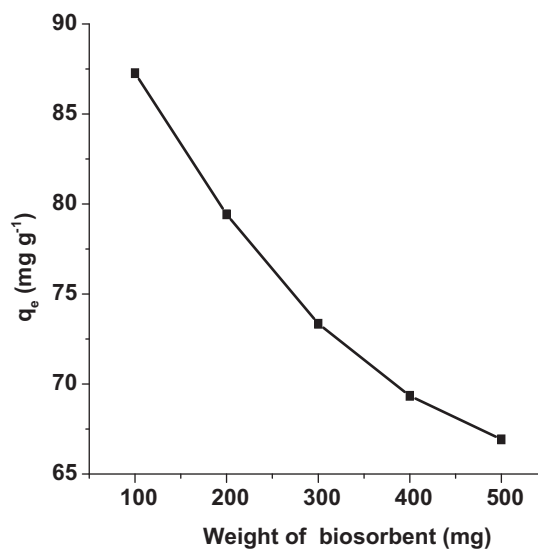


Figure 4 Amount of Cr(III) ion biosorbed q_e (mg/g) against various biosorbent weights. (Initial metal ion concentration: 200 mg/L, temperature: 298 K, agitation time: 3 h, agitation speed: 125 rpm.)

by ion-exchange (Li et al., 2007). At low pH values ($\text{pH} < \text{pH}_{\text{pzc}}$), the biosorbent surface is saturated with hydrogen ions, which reduces the uptake of Cr(III) ions because of competition between the Cr(III) ions and the hydrogen ions for the biosorbent active sites. Generally, metal biosorption involves a complex mechanism of ion exchange, chelation of metals with various anionic functional groups mainly hydroxyl, carboxyl, sulphhydryl, amino, sulfate, thiol, phosphate and others, biosorption by physical forces and ion entrapment in the inter and intrafibrillar capillaries and spaces of the cell

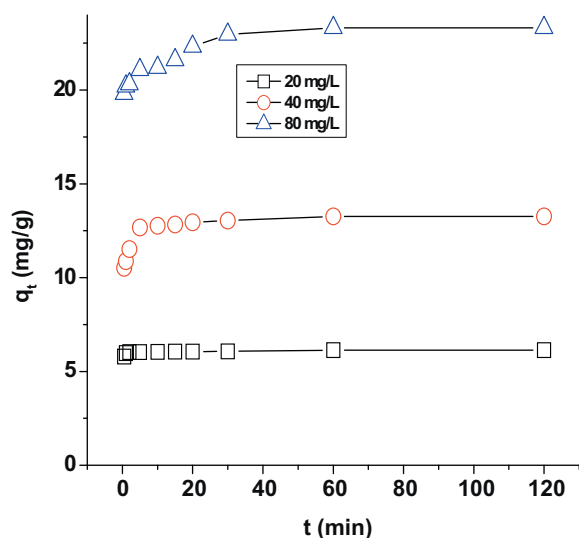


Figure 5a The non linear kinetic plots of q_t (mg/g) against time t (min) for various initial Cr(III) ion concentrations of 20, 40 and 80 mg/L. *N. diderrichii* seed biomass weight (NDS): 50 mg.

structural network of a biosorbent (Ofomaja and Ho, 2007; Parvathi et al., 2007; Pino et al., 2006).

3.3. Effect of biosorbent dose

Fig. 4 shows a linear relationship of Cr(III) ions biosorbed in mg/g of the NDS biosorbent with respect to the amount of Cr(III) adsorbed at equilibrium, q_e . An increase was observed in the amount of Cr(III) ion adsorbed with increasing biosorbent dose up till 500 mg after which there was a decline in the biosorption capacity of the NDS biosorbent. This can be attributed to a decrease in specific surface area and increase in diffusion path length because of the aggregation of the biosorbent particles. This aggregation becomes increasingly significant as the weight of the biosorbent is increased. However, there was increase in the percentage of Cr(III) ion adsorbed with increasing biosorbent dose (plot not shown). Similar trends have been reported by Shukla et al. (2002), Unuabonah et al. (2007) and Gupta and Bhattacharyya (2008).

3.4. Biosorption kinetics and equilibrium

Figs. 5a and 5b show the non linear kinetic plots of the amount of Cr(III) biosorbed, q_t (mg/g) against time t (min) at various initial Cr(III) concentrations and NDS weights respectively.

Both kinetic and equilibrium experimental data obtained from this study were fitted to various kinetic and equilibrium models. At initial concentrations of 20, 40 and 80 mg/L of Cr(III), the maximum biosorption was reached within 60 min. Five kinetic models (pseudo-first order, modified pseudo-first order, ion-exchange, pseudo-second order, and Elovich) were used to describe the experimental data obtained (Tables 1 and 2). It was observed from the correlation coefficient that the pseudo-second order gave better fit to the experimental data obtained from increasing initial metal ion concentration and increasing biosorbent weight, compared with other kinetic models. From the pseudo-second kinetic

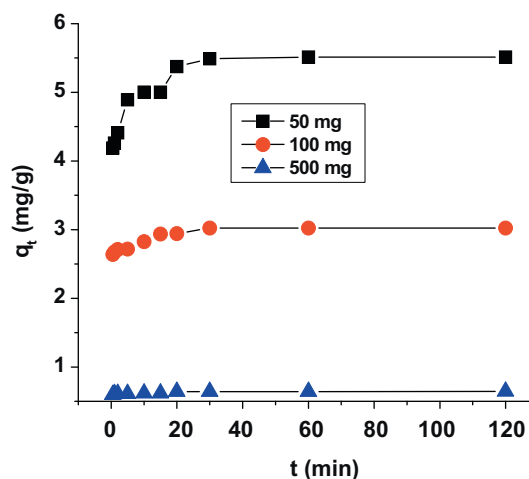


Figure 5b The non linear kinetic plots of q_t (mg/g) against time t (min) for various *N. diderrichii* seed biomass weights (NDS) of 50, 100 and 500 mg. (Initial Cr(III) ion concentration: 20 mg/L.)

Table 1 Parameters of various kinetic models for the biosorption of Cr(III) onto NDS biosorbent at various initial concentrations.

	20 mg/L	40 mg/L	80 mg/L
<i>Pseudo-second order</i>			
q_e (mg/g)	5.574	12.077	15.537
K_2 (g/mg min)	0.233	0.208	0.156
h (mg/g min)	7.239	30.338	37.658
R^2	1.000	1.000	1.000
<i>Pseudo-first order</i>			
q_e (mg/g)	2.044	1.217	2.160
K_1 (min^{-1})	0.022	0.026	0.012
R^2	0.820	0.788	0.958
<i>Elovich</i>			
β	21.322	1.865	1.395
α	$3.58\text{E} + 3$	$6.29\text{E} + 8$	$9.96\text{E} + 11$
R^2	0.764	0.889	0.940
<i>Ion-exchange model</i>			
S (min^{-1})	0.062	0.065	0.061
R^2	0.876	0.902	0.987
<i>Modified pseudo-first</i>			
q_e (mg/g)	0.521	3.904	8.654
K_3 (min^{-1})	0.062	0.063	0.058
R^2	0.877	0.917	0.986

data, initial sorption rates h increased with increasing initial Cr(III) ion concentration and decreased with increasing biosorbent weight. This is because more time will be required to biosorb Cr(III) ion as its concentration increases with constant biosorbent weight and less time will be required to biosorb Cr(III) ion as biosorbent weight increases due to an increase in the active sites of the biosorbent.

Also, as the initial Cr(III) concentration increased to 200 mg/L, maximum biosorption of 88.33 mg/g was achieved within 10 min. This indicates that the initial removal of Cr(III) ions from aqueous solution was very rapid at the beginning of the reaction due to external mass transfer of the solute onto the

Table 2 Parameters of various kinetic models for the biosorption of Cr(III) onto NDS biosorbents at various biosorbent masses.

	50 mg	100 mg	500 mg
<i>Pseudo-second order</i>			
q_e (mg/g)	5.543	3.032	0.644
K_2 (g/mg min)	0.232	0.202	0.156
h (mg/g min)	7.128	1.857	0.065
R^2	0.999	1.000	1.000
<i>Pseudo-first order</i>			
q_e (mg/g)	1.072	0.338	0.053
K_1 (min^{-1})	0.068	0.069	0.119
R^2	0.889	0.843	0.788
<i>Elovich</i>			
β	3.211	11.148	112.359
α	12.298	14.155	112.965
R^2	0.957	0.914	0.824
<i>Ion-exchange model</i>			
$S(\text{min}^{-1})$	0.067	0.030	0.052
R^2	0.888	0.843	0.788
<i>Modified pseudo-first order</i>			
q_e (mg/g)	2.440	1.169	0.136
K_3 (min^{-1})	0.064	0.108	0.117
R^2	0.895	0.921	0.786

Table 3 Various biosorbents used by researchers for the uptake of Cr(III) onto NDS.

Biosorbents	Biosorption capacities (mg/g)	References
Meranti sawdust	37.88	Rafatullah et al. (2009)
Activated carbon from apricot stone	29.30	Kobyas et al. (2005)
Water lily	6.11	Elangovan et al. (2008a,b)
Water hyacinth	6.61	Elangovan et al. (2008a,b)
Green taro	6.07	Elangovan et al. (2008a,b)
Mangrove leaves	6.54	Elangovan et al. (2008a,b)
Reed mat	7.18	Elangovan et al. (2008a,b)
<i>Spirulina</i> sp.	185.0	Chojnacka et al. (2005)
<i>N. diderrichii</i> seed biomass	483.81	This study

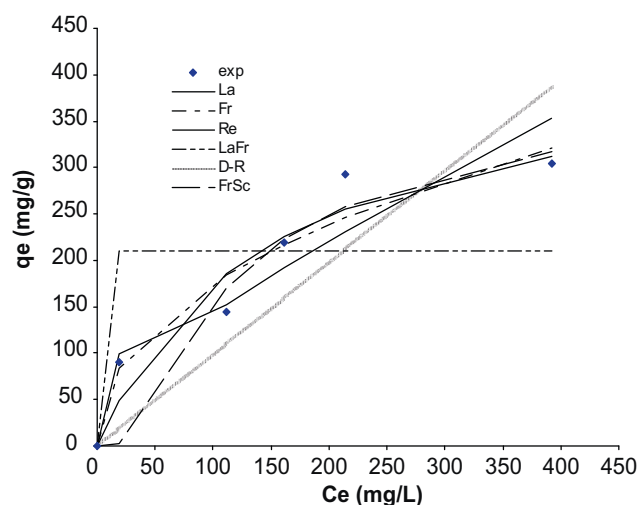
biosorbent surface and the rapid filling of the unoccupied active sites at the start of the reaction (Ofomaja and Unuabonah, 2011).

The kinetic data obtained from increase in biosorbent mass indicates that biosorption of Cr(III) onto NDS using pseudo-second order model, decreased from 5.543 to 0.644 mg/g respectively (Table 2). This may be a result of biosorbent agglomeration (Shukla et al., 2002; Unuabonah et al., 2007; Gupta and Bhattacharyya, 2008).

From Langmuir equilibrium data, the biosorption capacity of NDS was calculated to be 483.81 mg/g (Tables 3 and 4). This is very high compared with the values obtained from other biosorbents for Cr(III) uptake as shown in Table 3. Three two-parameter (Langmuir, Freundlich, and Dubinin–Radushkevich) and three three-parameter (Redlich–Peterson, Langmuir–Freundlich, and Fritz–Schlunder) equilibrium

Table 4 Isotherm parameters for the biosorption of Cr(III) onto NDS biosorbents.

NDS	La	Fr	D–R	Re	LaFr	FrSc
<i>Cr(III)</i>						
Parameters	2	2	2	3	3	3
q_{max} (mg/g)	483.81	23.00	405.56	0.012	210.18	1.16
AIC_c	47.02	46.12	50.43	70.93	78.75	76.87
λ_i	1.57	1.00	8.66	2.44×10^5	1.22×10^7	9.36×10^6
La = Langmuir model.						
Fr = Freundlich model.						
D–R = Dubinin–Radushkevich model.						
Re = Redlich–Peterson.						
LaFr = Langmuir–Freundlich Model.						
FrSc = Fritz–Schlunder three parameter model.						

**Figure 6** Model plots for the biosorption of Cr(III) onto *N. diderrichii* seed biomass (NDS). (Initial metal ion concentration: 200 mg/L, temperature: 298 K, agitation time: 3 h, agitation speed: 125 rpm.)

models were used to fit equilibrium data obtained. The Freundlich isotherm model was found to describe the data better than other models because of its least Akaike weight (λ_i). This implies that the NDS surface has heterogeneous sites for the adsorption of Cr(III) from aqueous solution. The Freundlich model is closely followed by the Langmuir isotherm model (Table 4). Fig. 6 shows the model plots for the biosorption of Cr(III) onto NDS. Again, the two-parameter models gave better fits to experimental than the three-parameter models. Similar observations were made by Akpa and Unuabonah (2011) and El-Khaiary and Malash (2011).

4. Conclusion

The sequestration of Cr(III) onto *N. diderrichii* seed biomass was investigated in this study. Characterization of the NDS biosorbent with FTIR showed that it possesses –OH functionality which is likely the main biosorption site for Cr(III). SEM images of NDS showed relatively large but irregular pores with a pore size of 3.986 nm and a pore volume of 0.00632 cm^3/g .

The specific surface of the NDS biosorbent from Nitrogen sorption analysis was $5.36 \text{ m}^2/\text{g}$ and its pH_{pzc} , 4.90.

Experimental data obtained were fitted to various kinetic and equilibrium models. Freundlich and pseudo-second order kinetic models gave better fit to experimental data. This NDS biosorption system gave a very high kinetic rate of uptake of Cr(III) with a high monolayer biosorption capacity which is relatively better than those of many biosorbents that had been previously used for Cr(III) removal from aqueous solution.

N. diderrichii seed biomass biosorbent is here recommended as a readily available, cheap and environmental friendly biosorbent which will serve as a good and cost effective alternative to activated carbon for the treatment of polluted water and industrial effluents.

Acknowledgments

The authors acknowledge the support of the Academy of Sciences for the Developing World and the Chinese Academy of Sciences (TWAS-CAS) for providing fellowship to Martins O. Omorogie at the National Center for Nanoscience and Technology, China, where this research was carried out. This work was also supported in part by the Natural Science Foundation of China (Nos. 21005023, 91123003) and the National Basic Research Program of China (No. 2011CB933401).

Appendix A. Supplementary data

Supplementary data associated with this article can be found, in the online version, at <http://dx.doi.org/10.1016/j.jscs.2012.09.017>.

Reference

- Abbas, M., Nadeem, R., Zafar, M.N., Arshad, M., 2008. Biosorption of chromium (III) and chromium (VI) by untreated and pretreated *Cassia fistula* biomass from aqueous solutions. *Water Air Soil Pollut.* 191, 139–148.
- Adeoye, A.O., Waigh, R.D., 1983. Secoiridoid and Triterpenic acids from the stems of *Nauclea diderrichii*. *Phytochemistry* 22 (4), 975–978.
- Akaike, H., 1974. A new look at the statistical model identification.. *IEEE Trans. Autom. Control* 19, 716–723.
- Akpa, O.M., Unuabonah, E.I., 2011. Small-sample corrected Akaike information c: an appropriate statistical tool for ranking of adsorption isotherm models. *Desalination* 272, 20–26.
- Anirudhan, T.S., Radhakrishnan, P.G., 2007. Chromium(III) removal from water and wastewater using a carboxylated-functionalized cation exchanger prepared from lignocellulosic residue. *J. Colloid Interface Sci.* 316, 268–276.
- Barrera, H., Urena-Nunez, F., Bilyeu, B., Barrera-Diaz, C., 2006. Removal of chromium and toxic ions present in mine drainage by *Ectodermis Opuntia*. *J. Hazard. Mater.* B136, 846–853.
- Bayramoğlu, G., Arica, M.Y., 2008. Adsorption of Cr(VI) onto PEI immobilized acrylate-based magnetic beads: isotherms, kinetics and thermodynamics study. *Chem. Eng. J.* 20, 20–28.
- Bozdoğan, H., 2009. Akaike's information criterion and recent developments in information complexity. *J. Math. Psychol.* 44, 62–91.
- Burnham, K.P., Anderson, D.R., 2004. Multimodel inference. understanding AIC and BIC in model selection. *Amsterdam Workshop on Model Selection*, August 27–29.
- Chen, T., Wise, S.S., Kraus, S., Shaffiey, F., Wise Dr, J.P., 2009. Particulate hexavalent chromium is cytotoxic and genotoxic to the North Atlantic right whale (*Eubalaena glacialis*) lung and skin fibroblasts. *Environ. Mol. Mutagen.* 50, 387–394.
- Chojnacka, K., Chojnacki, A., Gorecka, H., 2005. Biosorption of Cr^{3+} , Cd^{2+} and Cu^{2+} ions by blue-green algae *Spirulina* sp.: kinetics, equilibrium and the mechanism of the process. *Chemosphere* 59, 75–84.
- Cimino, G., Passerini, A., Toscano, G., 2000. Removal of toxic cations and Cr(VI) from aqueous solution by hazelnut shell. *Water Res.* 34, 2955–2962.
- Elangovan, R., Philip, L., Chandraraj, K., 2008a. Biosorption of chromium species by aquatic weeds; kinetics and mechanism studies. *J. Hazard. Mater.* 152, 100–112.
- Elangovan, R., Philip, L., Chandraraj, K., 2008b. Biosorption of hexavalent and trivalent chromium by palm flower (*Borassus aethiopum*). *Chem. Eng. J.* 141, 99–111.
- El-Khaiary, M.I., Malash, G.F., 2011. Common data analysis errors in batch biosorption studies. *Hydrometall.* 114, 1–7.
- Eren, E., Gumus, H., Sarihan, A., 2011. Synthesis, structural characterization and Pb(II) adsorption behavior of K- and H-birnessite samples. *Desalination* 279, 75–85.
- Garcia-Reyes, R.B., Rangel-Mendez, J.R., 2010. Adsorption kinetics of chromium(III) ions on agro-waste materials. *Bioresour. Technol.* 101, 8099–8108.
- Gayawan, E., Adebayo, S.B., Ipinyomi, R.A., Oyejola, B.A., 2010. Modeling fertility curves in Africa. *Demogr. Res.* 22, 211–236.
- Gobi, K., Mashitah, M.D., Vadivelu, V.M., 2011. Adsorptive removal of methylene blue using novel adsorbent palm oil mill effluent waste activated sludge: equilibrium, thermodynamics and kinetic studies. *Chem. Eng. J.* 171, 1246–1252.
- Gupta, S.S., Bhattacharyya, K.G., 2008. Immobilization of Pb(II) , Cd(II) and Ni(II) ions on kaolinite and montmorillonite surfaces from aqueous medium. *J. Environ. Manage.* 87 (1), 46–58.
- Howard, A.G., Khdary, N.H., 2005. Nanoscavenger based dispersion preconcentration; sub-micron particulate extractants for analyte collection and enrichment. *Analyst* 130, 1432–1438.
- Jacobs, A.J., Testa, S.M., 2004. Overview of chromium(VI) in the environment: background and history. In: Guertin, J., Jacobs, A.J., Avakian, C.P. (Eds.), *Chromium(VI) Handbook*. CRC Press Inc., Boca Raton, FL, pp. 1–21.
- Kang, S.Y., Lee, J.U., Kim, K.W., 2008. Biosorption of Pb(II) from synthetic wastewater onto *Pseudomonas aeruginosa*. *J. Environ. Pollut.* 1–4, pp. 195–02.
- Khdary, N.H., Howard, A.G., 2011. New solid-phase-nanoscavenger for the analytical enrichment of mercury from water. *Analyst* 136, 3004–3009.
- Khdary, N.H., Gassim, A.E., Howard, A.G., 2012. Scavenging of benzodiazepine drugs from water using dual-functionalized silica nanoparticles. *Anal. Methods* 4, 2900–2907.
- Koby, M., Demirbas, E., Senturk, E., Ince, M., 2005. Adsorption of heavy metal ions from aqueous solutions by activated carbon prepared from apricot stone. *Bioresour. Technol.* 96, 1518–1521.
- Kwon, E., Castald, M.J., 2008. Investigation of mechanisms of polycyclic aromatic hydrocarbons (PAHs) initiated from the thermal degradation of styrene butadiene rubber (SBR) in N_2 atmosphere. *Environ. Sci. Technol.* 42, 2175–2180.
- Li, Q., Zhai, J., Zhang, W., Wang, M., Zhou, J., 2007. Kinetic studies of adsorption of Pb(II) , Cr(III) and Cu(II) from aqueous solution by sawdust and modified peanut husk. *J. Hazard. Mater.* 141, 163–167.
- Li, J., Lin, Q., Zhang, X., Yan, Y., 2009. Kinetic parameters and mechanisms of the batch biosorption of Cr(VI) and Cr(III) onto *Leersia hexandra* Swartz biomass. *J. Colloid Interface Sci.* 333, 71–77.
- Malkoc, E., 2006. Ni(II) removal from aqueous solutions using cone biomass of *Thuja orientalis*. *J. Hazard. Mater.* B137, 899–08.

- Mutua, F.M., 1994. The use of the Akaike information criterion in the identification of an optimum flood frequency model. *Hydrol. Sci. J.* 93, 235–244.
- Ofomaja, A.E., Ho, Y.S., 2007. Effect of pH on cadmium biosorption by coconut copra meal. *J. Hazard. Mater.* B139, 356–362.
- Ofomaja, A.E., Naidoo, E.B., Modise, S.J., 2009. Removal of copper(II) from aqueous solution by pine and base modified pine cone powder as biosorbent. *J. Hazard. Mater.* 168, 909–917.
- Ofomaja, A.E., Unuabonah, E.I., 2011. Adsorption of 4-nitrophenol onto cellulosic material, mansonia wood sawdust and multistage batch adsorption process optimization. *Carbohydr. Polym.* 83, 1192–1200.
- Oliveira, E.A., Montanher, S.F., Andrade, A.D., Nobrega, J.A., Rollemberg, M.C., 2005. Equilibrium studies for the sorption of chromium and nickel from aqueous solutions using raw rice bran. *Proc. Biochem.* 40, 3485–3490.
- Oliveira, W.E., Franca, A.S., Oliveira, L.S., Rocha, S.D., 2008. Untreated coffee husks as biosorbent for the removal of heavy metals from aqueous solutions. *J. Hazard. Mater.* 155, 507–512.
- Parvathi, K., Nagendra, R., Nareshkumar, R., 2007. Lead biosorption on waste beer yeast by-product, a means to decontaminate effluent generated from battery manufacturing industries. *Electron. J. Biotechnol.* 10, 1–14.
- Pino, G.H., Mesquita, L.M.S., Torem, M.L., Pinto, G.A.S., 2006. Biosorption of cadmium by green coconut shell powder. *Miner. Eng.* 19, 380–387.
- Rafatullah, M., Sulaiman, O., Hashim, R., Ahmad, A., 2009. Adsorption of copper(II), chromium(III), nickel(II) and lead(II) ions from aqueous solutions by meranti sawdust. *J. Hazard. Mater.* 170, 969–977.
- Rajesh, N., Deepthi, B., Subramaniam, A., 2007. Solid phase extraction of chromium(VI) from aqueous solutions by adsorption of its ion-association complex with cetyltrimethylammoniumbromide on an alumina column. *J. Hazard. Mater.* 144 (1–2), 464–469.
- Rajesh, N., Mishra, B.G., Pareek, P.K., 2008. Solid phase extraction of chromium(VI) from aqueous solutions by adsorption of its diphenylcarbazine complex on a mixed bed adsorbent (acid activated montmorillonite–silica gel) column. *Spectrochim. Acta, A Mol. Biomol. Spectrosc.* 69 (2), 612–618.
- Romero-Gonzalez, J., Gardea-Torresdey, J.L., Peralta-Videa, J.R., Rodriguez, E., 2005. Determination of equilibrium and kinetic parameters of the adsorption of Cr(III) and Cr(VI) from aqueous solutions to *Agave lechuguilla* biomass. *Bioinorg. Chem. Appl* 3, 55–68.
- Sawalha, M.F., Peralta-Videa, J.R., Romero-Gonzalez, J., Gardea-Torresdey, J.L., 2006. Biosorption of Cd (II), Cr(III), and Cr(VI) by saltbush (*Atriplex canescens*) biomass: thermodynamic and isotherm studies. *J. Colloid Interface Sci.* 300, 100–104.
- Shukla, A., Zhang, Y.H., Dubey, P., Malgrave, J.L., Shukla, S.S., 2002. The role of sawdust in the removal of unwanted materials from water. *J. Hazard. Mater.* 95, 132–152.
- Sidiras, D., Batzias, F., Schroeder, E., Ranjan, R., Tsapatsis, M., 2011. Dye adsorption on autohydrolyzed pine sawdust in batch and fixed bed systems. *Chem. Eng. J.* 171, 883–896.
- Stumm, W., Morgan, J.J., 1996. *Aquatic Chemistry*, third ed. Wiley, New York, pp. 534–540.
- The International for Conservation of Nature (IUCN). (1998). *African Regional Workshop; Conservation and Sustainable Management of trees*, Zimbabwe.
- Unuabonah, E.I., Olu-Owolabi, B.I., Adebawale, K.O., Ofomaja, A.E., 2007. Adsorption of lead and cadmium ions from aqueous solutions by tripolyphosphate-impregnated Kaolinite clay. *Colloid Surf., A Physicochem. Eng. Aspects* 292, 202–211.
- Vinod, V.T.P., Sashidhar, R.B., Sukumar, A.A., 2010. Competitive adsorption of toxic heavy metal contaminants by gum kondagogu (*Cochlospermum gossypium*): a natural hydrocolloid. *Colloids Surf. B* 75, 490–495.
- Zhan, Y., Luo, X., Nie, S., Huang, Y., Tu, X., Luo, S., 2011. Selective separation of Cu(II) from aqueous solution with a novel Cu(II) surface magnetic ion-imprinted polymer. *Ind. Eng. Chem. Res.* 50, 6355–6361.
- Zubair, A., Bhatti, H.N., Hanif, M.A., Shafqat, F., 2008. Kinetic and equilibrium modeling for Cr(III) and Cr(VI) removal from aqueous solutions by *Citrus reticulata* waste biomass. *Water Air Soil Pollut.* 191, 305–318.